

# Post Print

## **Kinetic model of SiGe selective epitaxial growth using RPCVD technique**

M. Kolahdouz, L. Maresca, R. Ghandi, Ali Khatibi and H. Radamson

N.B.: When citing this work, cite the original article.

Original Publication:

M. Kolahdouz, L. Maresca, R. Ghandi, Ali Khatibi and H. Radamson, Kinetic model of SiGe selective epitaxial growth using RPCVD technique, 2010, ECS Transactions, (33), 6, 581-593.

<http://dx.doi.org/10.1149/1.3487589>

Copyright: Electrochemical Society

Postprint available at: Linköping University Electronic Press

<http://urn.kb.se/resolve?urn=urn:nbn:se:liu:diva-65701>

# Kinetic model of SiGe selective epitaxial growth using RPCVD technique

M. Kolahdouz, L. Maresca, R. Ghandi, A. Khatibi and H. H. Radamson

School of Information and Communication Technology, KTH (Royal Institute of Technology)  
Isafjordsg. 22-26, Electrum 229, 16640 Kista, Sweden  
Phone: +46-8-7904333 Fax: +46-8-7904300  
E-mail: [mkes@kth.se](mailto:mkes@kth.se)

## Abstract

Recently, selective epitaxial growth (SEG) of B-doped SiGe layers has been used in recessed source/drain (S/D) of pMOSFETs. The uniaxial induced strain enhances the carrier mobility in the channel. In this work, a detailed model for SEG of SiGe has been developed to predict the growth rate and Ge content of layers in dichlorosilane(DCS)-based epitaxy using a reduced-pressure CVD reactor. The model considers each gas precursor contributions from the gas-phase and the surface.

The gas flow and temperature distribution were simulated in the CVD reactor and the results were exerted as input parameters for Maxwell energy distribution. The diffusion of molecules from the gas boundaries was calculated by Fick's law and Langmuir isotherm theory (in non-equilibrium case) was applied to analyze the surface. The pattern dependency of the selective growth was also modeled through an interaction theory between different subdivisions of the chips. Overall, a good agreement between the kinetic model and the experimental data were obtained.

## Introduction

SiGe epitaxy growth has attracted attention in both micro- (1-3) and opto-electronics due to its low cost and feasibility. It has also benchmarked an area in strain engineering where bandgap tailoring is essential for the mobility enhancement (4-6). Tremendous experimental results have been presented on the growth and integration of SiGe layers for different applications, meanwhile, remarkably fewer reports are available about the modeling of the growth (7-9). This point is highlighted when selective epitaxial growth (SEG) faces pattern dependency in which the SiGe layer profile is affected by the pattern layout (10-17). During recent years, various methods have been proposed to decrease the pattern dependency in SEG of SiGe layers but an effective method which completely eliminates this problem has not yet been presented (17).

Bodnar et al (10) proposed that the pattern dependency can be reduced remarkably by applying high HCl partial pressure. The drawback of this technique is the low growth rate due to the high etch rate of HCl gas. This phenomenon creates high defect density in the grown epilayer. Loo et al (14) suggested the combination of low growth pressure (10 torr) and high H<sub>2</sub> carrier gas (40 slm) to tackle the pattern dependency problem. However, the high H<sub>2</sub> flux makes it difficult to grow SiGe layers with high Ge content or high doping level.

This work, introduces an empirical model for the selective epitaxial growth of SiGe layers in a reduced pressure chemical vapor deposition reactor. The model takes into account gas and surface kinetics and reactions for the growth rate and Ge composition calculation. Pattern dependency has also been evaluated through the modeling of gas consumption in a certain chip and the interaction between chips on the wafer. In fact, this model has the capability to provide growth rate and Ge composition data on a 2-dimensional epitaxy mask.

### Experimental Details

The epitaxial layers were grown on blanket or patterned Si(100) substrates in an ASM Epsilon 2000 RPCVD reactor at different temperatures and pressures. Dichlorosilane ( $\text{SiH}_2\text{Cl}_2$ ) and 10% germane ( $\text{GeH}_4$ ) in  $\text{H}_2$  were used as Si and Ge sources, respectively. HCl was utilized as the etchant to obtain selectivity during the epitaxy. In order to verify the model, different partial pressures of  $\text{SiH}_2\text{Cl}_2$  ( $P_{\text{DCS}}$ ),  $\text{GeH}_4$  ( $P_{\text{GeH}_4}$ ) and HCl ( $P_{\text{HCl}}$ ) were applied while 150nm oxide layer was used as the mask against Si.

The substitutional Ge content and the layer thickness of SiGe layers were measured directly by high resolution x-ray diffraction (HRXRD) for the blanket wafers. For the measurements on the pattern substrates, the x-ray beam was focused on arrays of openings with the same size. In order to obtain adequate beam intensity, a mirror was applied in the primary optics and long acquisitions were performed to generate high quality rocking curves. No thickness fringes were observed in the rocking curves to estimate the layer thickness in the openings. The Ge content was obtained from simulation of the rocking curves by using the Takagi-Taupin equations. Atomic force microscopy (AFM) and cross-sectional high resolution scanning electron microscopy (HRSEM) were employed to measure the layer thickness of the grown SiGe layers inside the oxide openings.

In this study, the PHOENICS-CVD simulation program has been used to determine the gas kinetics in the CVD chambers for different total pressures (10, 20 and 40 torr) and temperature distribution during epitaxy. The simulation provided essential information about the gas boundaries which is a very important parameter for the modeling of the epitaxy process.

### Results and Discussion

#### Theory of selective epitaxy of SiGe layers

The kinetics of CVD growth can physically be described by classical boundary layer theory assuming a laminar gas flow over the wafer. Figure 1 illustrates a schematic view of the gas kinetics.

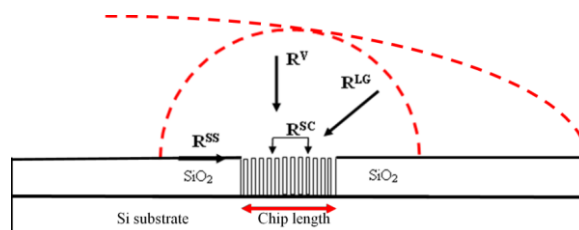


Figure 1. Schematic illustration of how a classical boundary layer is produced from laminar gas stream flowing over the wafer in SEG during the CVD process. In this figure, black arrows demonstrate different ways through which diffused molecules from the boundary reach the dangling bonds.

Due to the frictional force between the gas steam and the stationary susceptor/substrate, a stagnant boundary layer is established during the gas flow (see Figure 1). Beyond this boundary layer, the gas is assumed to be well-mixed and moving at a constant speed. Gas molecules which have diffused through the gas boundary layer, eventually reach the substrate surface. They are attracted towards the dangling bonds and are then consumed. The vertical diffusion path of the gas molecules was 10-15 mm for the total pressure of 20-40 torr in an Epsilon CVD reactor (16). In the case of a chip with opening arrays, a virtual volume is established as shown in Figure 1.

The gas-phase depletion for the patterned substrate occurs both vertically and laterally around a single chip. Inside the chip depletion volume, there are four different sources of species which contribute to selective epitaxy growth:

- Vertical gas-phase diffusion
- Lateral gas-phase diffusion
- Surface diffusion from the surrounding oxide (or nitride)
- Surface diffusion from the chip oxide

For each of the inlet sources, the identified components contribute to the total growth rate ( $R_{tot}$ ) in the following expression:

$$R_{Tot} = R_{Si}^V + R_{Si}^{LG} + R_{Si}^{SS} + R_{Si}^{SC} + R_{Ge}^V + R_{Ge}^{LG} + R_{Ge}^{SS} + R_{Ge}^{SC} - R_E^V - R_E^{LG} - R_E^{SS} - R_E^{SC} \quad [1]$$

$R^V$  and  $R^{LG}$  relate to the incoming gas molecules in vertical and lateral direction, while  $R^{SS}$  and  $R^{SC}$  represent the components derived from the dissociated reactant molecules on the oxide surface outside or within a chip.  $R_E$  is the etch rate of the etchant species.

### Temperature distribution

The kinetic of the gas molecules is dependent on both temperature and growth pressure. Therefore, the temperature distribution for an ASM Epsilon 2000 RPCVD reactor was simulated using PHOENICS-CVD software at three different growth pressures: 10, 20 and 40 torr.

In order to simplify the process, hydrogen was considered as the main gas stream passing above the susceptor (and wafer). According to the deposition recipe, a 20 slm (standard litter per minute)  $H_2$  inlet flow was applied. In Epsilon 2000 reactor, growth temperature is controlled through the assembly of lamps which heat up the susceptor; this heat is then transferred to the flowing gas (650°C). Figure 2 demonstrates the temperature distribution in the flow direction at the center of the reactor for 10 and 40 torr total pressures.

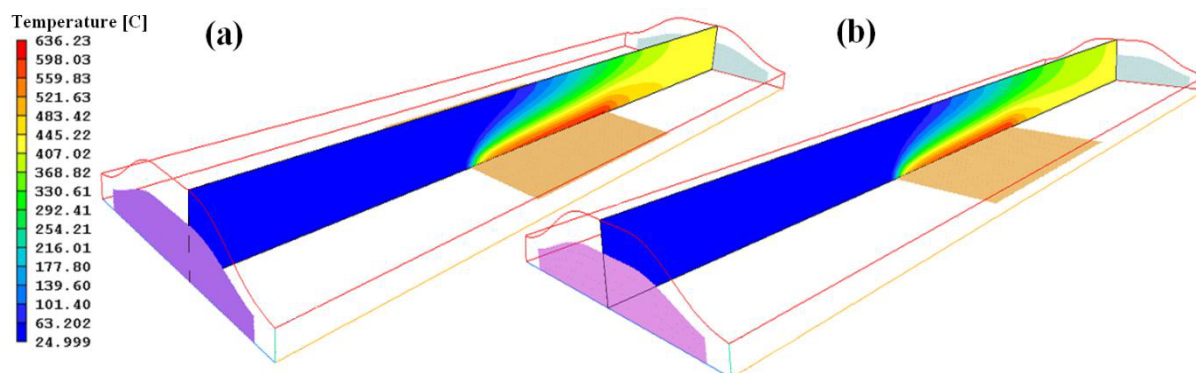


Figure 2. Side view illustration of the temperature profile simulated in a) 40 torr and b) 10 torr. The purple, grey and orange colors represent the inlet, outlet and the susceptor areas, respectively.

It can be observed from the figure that by decreasing the growth pressure, the velocity of the gas increases and this affects the temperature distribution inside the chamber. Moreover, by decreasing the growth pressure the formed gas boundary moves closer to the substrate and subsequently the number of diffusing molecules decreases (17). It is worth mentioning that during the deposition, the susceptor rotates and therefore a uniform temperature distribution is obtained.

### Gas distribution

In CVD process, the partial pressure of the reactant gas is adjusted by the mass flow controller. Since most of the introduced gases flow over the substrate, the gas flow which reaches the substrate is not the same as the input value. Therefore, only a fraction of the total gas flow diffuses downwards to the dangling bonds ( $F_{to}$ ). In this case, for a Si opening in a chip, the following fluxes are defined:

$$F_S = -D\nabla C_P \quad \text{Fick's law} \quad [2]$$

$$F_{to} = 2F_S\pi r^2 \quad [3]$$

where  $F_S$  is the flux per unit area (see Figure 3) on the depletion volume of each opening (16) and  $C_P$  is the species concentration in the flux. The Si dangling bonds in an oxide opening consume the gas molecules, creating a force which attracts the gas molecules towards the openings. The species concentration as a function of distance from the opening can be obtained by combining Eq.2 and Eq.3 which leads to:

$$C_p(r) = C_\infty - \frac{K}{r} \quad \text{where: } K = \frac{F_{to}}{2\pi D} \quad [4]$$

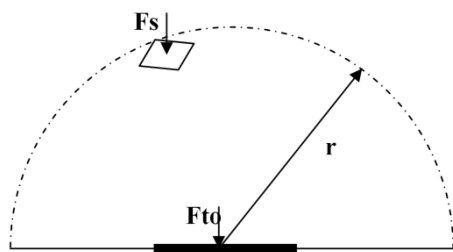


Figure 3. A schematic sketch of the flux of molecules over an opening in a spherical symmetric

This can be applied to define a function for the depletion power of an opening on the coming molecules. It can be concluded from Eq. 4 that by moving closer to the openings, the species concentration decreases. This reduction, which originates from the opening depletion power, is the main reason for the movement of species inside the stationary region.

### Modeling of the SEG of SiGe on non-patterned substrates

Vertical growth components. The vertical parameters in eq. 1 are identified with the growth on the blanket wafer where no lateral diffusion exists. There are a series of publications about the epitaxial growth of SiGe layers using the CVD technique. The Meng Tao approach (18) is presented here as a basis for the upcoming model regarding growth rate in SEG of SiGe. In Tao's model, the impinging reactant molecules on the Si surface are incorporated to the dangling bonds. By applying the Maxwell distribution function in unit time, the number of the reactant molecules

( $d\Gamma$ ) which interact with a unit area of the substrate with kinetic energy between  $E_K$  and  $E_K + dE_K$  can be thus estimated:

$$d\Gamma = 8\pi N_R \left( \frac{1}{2\pi m_R k_b T} \right)^{\frac{3}{2}} m_R E_K \exp\left(-\frac{E_K}{k_b T}\right) dE_K \quad [5]$$

where  $N_R$  is the number of reactant molecules in a unit volume of the gas phase and  $m_R$  is the mass of a reactant molecule. Integrating the formula from  $E_A$  (deposition activation energy) to  $+\infty$ , the number of the activated reactant molecules which strike a unit area of the substrate in a unit time is given by:

$$\Gamma = \frac{N_R}{(2\pi m_R k_b T)^{\frac{1}{2}}} (E_A + k_b T) \exp\left(-\frac{E_A}{k_b T}\right) \quad [6]$$

The deposition of Si layers on a Si surface is notably the simplest case of epitaxial growth. The growth rate for Si deposition can be calculated as follows:

$$R = \frac{\Gamma}{N_0} = \beta \frac{(1 - \theta_{H(Si)} - \theta_{Cl(Si)})}{N_0} \frac{P_{SiH_2Cl_2}}{(2\pi m_{SiH_2Cl_2} k_b T)^{\frac{1}{2}}} \left( \frac{E_{SiH_2Cl_2}}{k_b T} + 1 \right) \exp\left(-\frac{E_{SiH_2Cl_2}}{k_b T}\right) \quad [7]$$

where  $\beta$ ,  $\theta$ ,  $P$ ,  $m$ ,  $N_0$  and  $E$  are respectively: unit-less constant; surface coverage of hydrogen or chlorine; partial pressure of DCS; molecular mass of DCS; number of atoms in a unit volume of the substrate layer; and activation energy needed for deposition. The constant  $\beta$  is considered as a tooling factor which is reactor- and gas-dependant. It must be calibrated for each CVD reactor.

At temperatures lower than 900 °C, a high percentage of surface sites are blocked by Cl(s) and H(s); whereas at temperatures above 900 °C almost all sites become available (19). Hydrogen desorbs at a much lower temperature than does chlorine; this explains the smaller growth rates achieved in chlorine-based Si-epitaxy compared to that of hydrogen.

The surface coverage temperature dependency of an adsorbed gas can be obtained through Langmuir isotherm. For Si deposition, the dominant reactions occur through a series of Cl dissociation but ultimately the following chemical reaction and adsorption can be written:



The Langmuir isotherm for an equilibrium case can be written as:

$$B(T) = \frac{\theta_{Cl}^2}{P(1 - \theta_{Cl})^2} \quad [8]$$

where  $B$  is the reaction constant and  $P$  is DCS partial pressure. However, epitaxy is a non-equilibrium process on account of which the above expression must be thus modified:

$$\theta_{Cl} = \frac{1}{1 + \sqrt{B(T) \times P^{-4.5}}} \quad [9]$$

This expression provides the chlorine coverage on the Si surface for different temperatures during the growth of Si from the DCS source. According to previous reports in the temperature range used for SEG of SiGe layers (600-725), hydrogen occupies less than 5% of the sites. This value ( $\theta_H = 5\%$ ) has been applied to the whole deposition range in the model (19).

In order to obtain selectivity during growth, HCl gas is introduced to remove the undesirable nuclei on the oxide (or nitride) surface. At the same time, the deposited Si layer in the openings is etched which decreases the original growth rate. The growth rate equation for Si deposition in presence of HCl is given by:

$$R_T = R_{Si}^V - R_E^V \quad [10]$$

$$R_T = \beta \frac{(1 - \theta_{H(Si)} - \theta_{Cl(Si)})}{N_0} \frac{P_{SiH_2Cl_2}}{(2\pi m_{SiH_2Cl_2} k_b T)^{\frac{1}{2}}} \left( \frac{E_{SiH_2Cl_2}}{k_b T} + 1 \right) \exp\left(-\frac{E_{SiH_2Cl_2}}{k_b T}\right) \quad [11]$$

$$- \frac{\gamma}{N_0} \frac{P_{HCl}^{0.596}}{(2\pi m_{HCl} k_b T)^{\frac{1}{2}}} \left( \frac{E_{Etching}}{k_b T} + 1 \right) \exp\left(-\frac{E_{Etching}}{k_b T}\right)$$

where  $\gamma$  is another unit-less constant which includes the gas properties and gas distribution in a CVD chamber. The activation energy of etching is 37.5 Kcal/mol. This value is between 22 and 44 Kcal/mol which is the energy needed to break one and two Si-Si bonds. This proves that compared to bulk Si atoms, Cl is able to remove adsorbed Si atoms (before they become incorporated in the Si lattice) more easily. Experimental results show that the dependency of etch rate on  $P_{HCl}$  is actually not linear. Instead, a sublinear relationship ( $P_{HCl}^{0.596}$ ) is observed. This discrepancy is caused by the migration of Cl atoms on the Si surface. For the SEG of SiGe layers,  $GeH_4$  precursor has been added to the reactant gases. In this case, eq.1 changes as follows:

$$R_T = R_{Si}^V + R_{Ge}^V - R_E^V \quad [12]$$

The presence of Ge atoms on the surface enhances the growth rate for two reasons; first, they require lower activation energy for deposition than do Si (0.61 eV for Ge compared to 2.08 eV for Si); and second, the desorption energy of other species (e.g. H and Cl) from these atoms is also lower than Si which makes them favorable desorption sites for undesired atoms on the surface. Thus, Si atom binding becomes easier in the presence of Ge atoms. This can emerge through the coefficient “m” in the total growth rate equation.

Therefore, eq.12 can be modified for SiGe growth in presence of HCl as:

$$R_T = R_{Si/Si}^V + R_{Ge/Ge}^V + R_{Si/Ge}^V - R_E^V = R_{Si/Si}^V + R_{Ge/Ge}^V + mR_{Ge/Ge}^V - R_E^V \quad [13]$$

where m is called the substitution coefficient. Theory must now be added in the form of effective reaction rate constants. In this way growth rates are related to chemical reaction kinetics:

$$R_T = \beta \frac{(1 - \theta_{H(Si)} - \theta_{Cl(Si)})}{N_0} \frac{P_{GeH_4}}{(2\pi m_{SiH_2Cl_2} k_b T)^{\frac{1}{2}}} \left( \frac{E_{SiH_2Cl_2 \text{ on } Si}}{k_b T} + 1 \right) \exp\left(-\frac{E_{SiH_2Cl_2 \text{ on } Si}}{k_b T}\right) \quad [14]$$

$$+ \chi \frac{(1 + m)(1 - \theta_{H(Si)} - \theta_{Cl(Si)})}{N_0} \frac{P_{GeH_4}}{(2\pi m_{GeH_4} k_b T)^{\frac{1}{2}}} \left( \frac{E_{GeH_4 \text{ on } Si}}{k_b T} + 1 \right) \exp\left(-\frac{E_{GeH_4 \text{ on } Si}}{k_b T}\right)$$

$$- \frac{\gamma}{N_0} \frac{P_{HCl}^{0.596}}{(2\pi m_{HCl} k_b T)^{\frac{1}{2}}} \left( \frac{E_{Etching}}{k_b T} + 1 \right) \exp\left(-\frac{E_{Etching}}{k_b T}\right)$$

where  $\chi$  is a unit-less constant which is dependent on the gas property. The m coefficient is suggested to be the number of silyl groups which have been substituted for hydrogen atoms in germane molecules by a chemical gas reaction ( $0 \leq m \leq 4$ ). In the range  $600^\circ\text{C} \leq T \leq 725^\circ\text{C}$ , it is reported (20) that the deposition degree of germane-hydrogen substitution is fixed by  $m = 2$ .

Since the SiGe layers contain a compressive strain, the bonding energy becomes weaker. As a result, the activation energy of the etching will decrease by increasing the Ge content (or strain). The experimental data demonstrate the following expression for etching activation energy:

$$E_{Etching} = 1.5473e^{-12.535P_{GeH_4}} \quad [15]$$

Although an increase in the etch rate is observed in SiGe epitaxy, its growth rate is still higher compared to that of Si.

The Ge content in SiGe layers is also an important factor which is obtained from the flux/partial pressure ratio between Ge and Si (21) as shown in the following equation:

$$\frac{x^2}{1-x} = \alpha \exp\left(\frac{0.7eV}{k_bT}\right) \left(\frac{P_{GeH_4} - (1-\lambda)P_{HCl}}{P_{SiH_2Cl_2} - \lambda P_{HCl}}\right) \quad [16]$$

where  $x$  and  $\alpha$  are the Ge content and the tooling factor, respectively.  $\lambda$  is a reaction fraction for Cl which indicates the interaction amount of Cl with Si and Ge. In the presence of HCl during selective epitaxy, Cl atoms preferably remove Si atoms rather than Ge ones. This parameter ( $\lambda$ ) is in a range between 0.9 and 1 depending on the HCl amount during epitaxy. The results of this study show that  $\lambda$  is close to 1 when the partial pressure of HCl is low (less than the Si source) and close to 0.9 for high HCl amount.

#### SEG on the global patterned substrate

Lateral components. As mentioned earlier, in selective epitaxy growth there are four different sources which depending on the layout, are either active or not. In order to evaluate a global chip design, wafers were processed with a single chip repeatedly patterned over an entire wafer. Nine different globally patterned wafers were processed; one wafer for each exposed Si coverage ranging from 0.01% to 37.85%. The openings inside chips were either 1×1, 2×2, 4×4, 8×8, 10×10, 20×20, 40×40, 80×80 or 160×160  $\mu\text{m}^2$  which were spaced 100  $\mu\text{m}$  apart. In these patterns, source c (Surface diffusion from the surrounding oxide) can be excluded from the deposition sources cited before. Thus, for each atom, three sources are available for deposition. For Si selective epitaxy, eq.1 can be rewritten as:

$$R_T = R_{Si}^V + R_{Si}^{LG} + R_{Si}^{SC} - R_E^V - R_E^{LG} - R_E^{SC} \quad [17]$$

LG and SC refer to the lateral gas and surface diffusion. In global patterns, depletion volumes of the chips are overlapped. However, for a global pattern with identical chips, the depletion power of the chips is similar; therefore, in this pattern, the lateral gas-phase diffusion contribution does not exist (see Figure 4). In this case, due to presence of Cl atoms on the oxide, the surface diffusion of Si atoms to the openings is negligible.

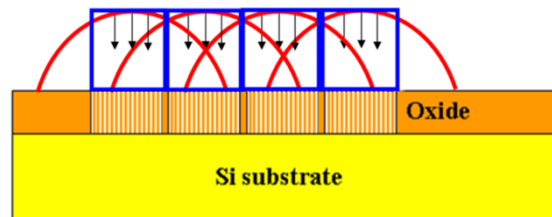


Figure 4. Schematic cross-sectional view of the boundary theory and gas diffusion in the global pattern. The sources available for deposition are “vertical component” and “diffusion from the oxide surface”.

The total growth rate equation for a global mask pattern is then:

$$R_T = R_{Si}^V - R_E^V - R_E^{SC} \quad [18]$$

Figure 5 illustrates the growth rate results obtained by AFM on nine different wafers. Pattern dependency in Si deposition follows the inverse order of SiGe (22). The last point in the chart with 100% exposed Si coverage is in fact the result of the same growth recipe on a blanket substrate which follows the similar order. As illustrated in the figure, growth rate rises when the exposed Si coverage increases. This is due to the decrease in the third part of eq.18. By decreasing the exposed Si coverage of the chip, which also means increasing its oxide coverage, the number of Cl atoms on the oxide surface increases. This enhances the etch rate inside the opening.

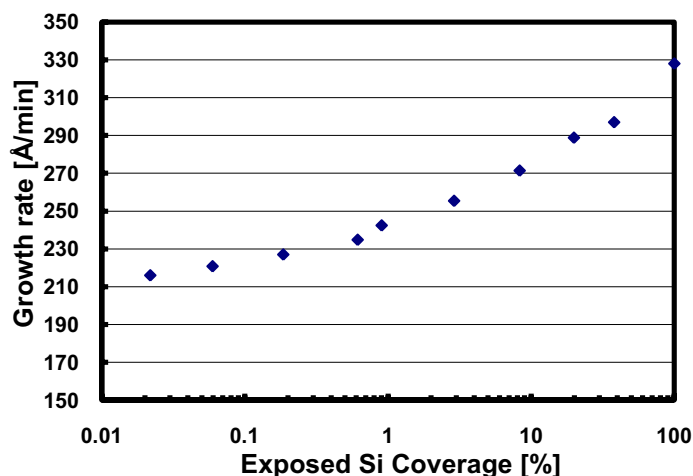


Figure 5. Illustration of growth rate vs. exposed Si coverage of the chip for nine different globally patterned wafers at 20torr total pressure. The applied  $P_{DCS}$  and  $P_{HCl}$  partial pressures were 120 and 20 mtorr, respectively

In SEG of Si,  $P_{HCl}^{SC}$  is provided through the diffusion of Cl atoms on the oxide surface and has an inverse relation with the exposed Si coverage of the chip. This can be shown as:

$$\Delta P_{HCl}^{SC} = -AP_{HCl} \frac{\Delta c}{c} \quad [19]$$

where  $c$  is the exposed Si coverage of the chip and  $A$  is a layout factor which can vary depending on the mask type used for isolation. By integrating eq. 19 and using a boundary condition the following equation is achieved:

$$P_{HCl}^{SC} = AP_{HCl} \ln \left( \frac{1}{c} \right) \quad [20]$$

Therefore, Eq 18 can be rewritten as follows:

$$R_T = \beta \frac{(1 - \theta_{H(Si)} - \theta_{Cl(Si)})}{N_0} \frac{P_{SiH_2Cl_2}}{(2\pi m_{SiH_2Cl_2} k_b T)^{\frac{1}{2}}} \left( \frac{E_{SiH_2Cl_2 on Si}}{k_b T} + 1 \right) \exp \left( - \frac{E_{SiH_2Cl_2 on Si}}{k_b T} \right) \quad [21]$$

$$- \frac{\gamma}{N_0} \frac{P_{HCl}^{0.596}}{(2\pi m_{HCl} k_b T)^{\frac{1}{2}}} \left( \frac{E_{Etching}}{k_b T} + 1 \right) \exp \left( - \frac{E_{Etching}}{k_b T} \right)$$

$$-\frac{\gamma}{N_0} \frac{(AP_{HCl} \ln(1/c))_{HCl}^{0.596}}{(2\pi m_{HCl} k_b T)^{\frac{1}{2}}} \left( \frac{E_{Etching}}{k_b T} + 1 \right) \exp\left(-\frac{E_{Etching}}{k_b T}\right)$$

SEG of SiGe on the global patterned substrate

In this part of the experiment, DCS, GeH<sub>4</sub> and HCl have been introduced for deposition on the patterned wafer. Thus, eq.1 can be rewritten as:

$$R_T = R_{Si}^V + R_{Si}^{LG} + R_{Si}^{SC} + R_{Ge}^V + R_{Ge}^{LG} + R_{Ge}^{SC} - R_E^V - R_E^{LG} - R_E^{SC} \quad [22]$$

In global masks with identical chips, lateral gas-phase diffusion of Si, Ge and Cl atoms are vanished (see Figure 4). Due to the presence of Ge atoms on the surface of the oxide, Cl desorption occurs from Ge atoms on the oxide surface and therefore, the surface diffusion of Cl becomes insignificant. Eq. 22 can then be rewritten as:

$$R_T = R_{Si}^V + R_{Ge}^V + R_{Ge}^{SC} - R_E^V = R_T^{Blanket} + R_{Ge}^{SC} \quad [23]$$

The Ge surface diffusion from the oxide surface has been written in the same form as that of Cl (eq.20). This can be referred to as the oxide surface contribution in Ge partial pressure ( $P_{Ge}^{SC}$ ):

$$P_{Ge}^{SC} = BP_{GeH_4} \ln\left(\frac{1}{c}\right) \quad [24]$$

where B is a unit-less constant dependent on the architecture of the mask (oxide or nitride) and c is the exposed Si coverage of the chip. The activation energy for Ge atoms to migrate on the oxide surface is 0.1 eV which must be added to the activation energy of the growth. Thus, the total growth rate equation will be:

$$\begin{aligned} R_T = & \beta \frac{(1 - \theta_{H(Si)} - \theta_{Cl(Si)})}{N_0} \frac{P_{GeH_4}}{(2\pi m_{SiH_2Cl_2} k_b T)^{\frac{1}{2}}} \left( \frac{E_{SiH_2Cl_2 on Si}}{k_b T} + 1 \right) \exp\left(-\frac{E_{SiH_2Cl_2 on Si}}{k_b T}\right) \\ & + \chi \frac{(1 + m)(1 - \theta_{H(Si)} - \theta_{Cl(Si)})}{N_0} \frac{P_{GeH_4}}{(2\pi m_{GeH_4} k_b T)^{\frac{1}{2}}} \left( \frac{E_{GeH_4 on Si}}{k_b T} + 1 \right) \exp\left(-\frac{E_{GeH_4 on Si}}{k_b T}\right) \\ & + \chi \frac{(1 + m)(1 - \theta_{H(Si)} - \theta_{Cl(Si)})}{N_0} \frac{(BP_{GeH_4} \ln(1/c))}{(2\pi m_{GeH_4} k_b T)^{\frac{1}{2}}} \left( \frac{E_{GeH_4 on Si} + 0.1eV}{k_b T} + 1 \right) \exp\left(-\frac{E_{GeH_4 on Si} + 0.1eV}{k_b T}\right) \\ & - \frac{\gamma}{N_0} \frac{P_{HCl}^{0.596}}{(2\pi m_{HCl} k_b T)^{\frac{1}{2}}} \left( \frac{E_{Etching}}{k_b T} + 1 \right) \exp\left(-\frac{E_{Etching}}{k_b T}\right) \end{aligned} \quad [25]$$

The Ge partial pressure from the oxide surface should be added to the vertical Ge partial pressure to extract the Ge composition. Eq. 16 can then be rewritten as:

$$\frac{x^2}{1-x} = \alpha \exp\left(\frac{0.7eV}{k_b T}\right) \left( \frac{P_{GeH_4} + (BP_{GeH_4} \ln(1/c)) - (1-\lambda)P_{HCl}}{P_{SiH_2Cl_2} - \lambda P_{HCl}} \right) \quad [26]$$

In Figure 6, model and experiment results are shown for proof of sanity. As it is perceived there is a good agreement between the model and the experiment for globally patterned wafers.

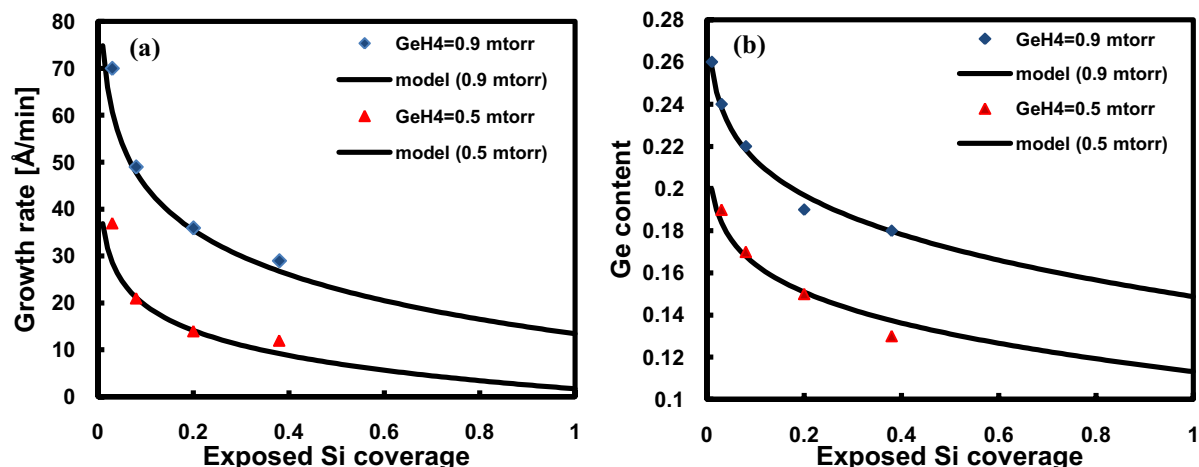


Figure 6. A) Growth rate vs. chip exposed Si coverage and B) Ge content vs. chip exposed Si coverage for different globally patterned wafers at 20 torr total pressure. The applied  $P_{\text{DCS}}$  and  $P_{\text{HCl}}$  partial pressures were 60 and 20 mtorr, respectively.  $P_{\text{GeH}_4}$  partial pressures were 0.9 and 0.5 mtorr.

#### SEG of SiGe on a non-uniform pattern

So far in this study, wafers have been uniformly patterned with same chip repeated all over the wafer. But in reality, the fabrication dies include chips with different exposed Si coverage (different opening sizes and densities). In order to develop the model for a real pattern, the interaction between the openings and chips must be taken into account.

As discussed earlier, there is a driving force  $f$ , for the species to be attracted to the dangling bonds inside the openings. This attraction force is strong close to an opening and decays gradually further away as an inverse function of distance (estimated by  $K/r$  where  $r$  is distance and  $K$  is a constant). Since a chip contains many openings then the driving force over species will be exerted non-linearly depending on the coverage of exposed silicon areas of the chip,  $c$ . In this case, the driving force equation for an array opening in a chip can be expressed by:

$$\iint f(x,y) dx dy = \alpha Kc + \beta K\sqrt{c} \quad [27]$$

where the linear and non-linear terms are calculated as  $\alpha = 0.24649$  and  $\beta = 1.1186$ . Using this equation, one can calculate the effects of chips on the diffused molecule from the boundary layer. By increasing the exposed Si coverage of the chip, the lateral gas-phase attraction of the diffused molecules increases. These molecules coming laterally in the gas-phase will be consumed by openings located along a distance of  $5\tau$  from the edge of the chip. As the exposed Si coverage of the chip increases, the  $\tau$  value decreases. The chip consumption length ( $\tau$ ) is defined as follows:

$$\tau = \frac{1}{\alpha Kc + \beta K\sqrt{c} + \delta} \quad [28]$$

where  $\delta$  is added to consider the collisions between the species before arriving at the consumption sites. The above equation demonstrates that by increasing the exposed Si coverage on chips with uniform patterns, the migration length of the gas molecules above the chip decreases. These

molecules are mostly consumed in openings closer to the edge of the chip. Empirical calculations showed that with the following numbers the best results were achieved for this model:

$$K\alpha = 0.0004 \mu\text{m}^{-1} \quad K\beta = 0.0011 \mu\text{m}^{-1} \quad \delta = 0.00048 \mu\text{m}^{-1}$$

In order to finalize the model for SEG of SiGe, another mask was designed and utilized to establish a model for interaction between the chips (see Figure 7). The main idea of the modeling is based on the non-uniform gas consumption among the chips. During growth, the chip with more exposed Si coverage attracts the gas molecules from the vertical component of the surrounding chips (so-called a trap-chip). On the mask for this study, the Si coverage of the surrounding chips (1%, 2.7% and 8% exposed Si coverage) were smaller than that of the central chip (2.7%, 8%, 19.75% and 37.85% exposed Si coverage).

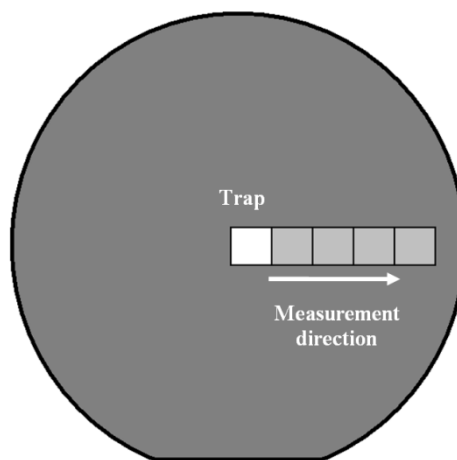


Figure 7. The mask design used to establish the interaction model between the chips

The trap-chip has a strong influence on the surrounding chips; however, the chips which are positioned far enough don't feel the presence of the trap. Thus, the growth rate as a function of distance from the trap ( $R_T(d)$ ) is expressed in the following manner:

$$R_T(d) = R_{Trap} + (R_{Surr} - R_{Trap}) \left(1 - e^{\frac{-d}{\tau(c_{surr})}}\right) \quad [29]$$

where  $d$  is the distance from the trap-chip and  $c_{Surr}$  is the exposed Si coverage of the surrounding chips. In this equation, the exponential function determines the interaction between the chips; the variable  $\tau$  is a function of exposed Si coverage (see eq. 28). The input parameters  $R_{TRAP}$  and  $R_{SURR}$  can be obtained from eq. 25 in different cases. The growth rate results of the experiment and the interaction model are demonstrated in Figure 8. As it has been shown in Figure 7, the trap-chip is surrounded by chips on the right and by oxide on other directions. Openings close to the trap are significantly impacted by the depletion volume of the trap-chip. In this volume, many of the gas molecules either in the gas-phase or on the surface are consumed by the trap-chip and thus the number of molecules available for the surrounding chips is reduced considerably. The trap-chip has no influence on the growth rate of openings positioned far away from it.

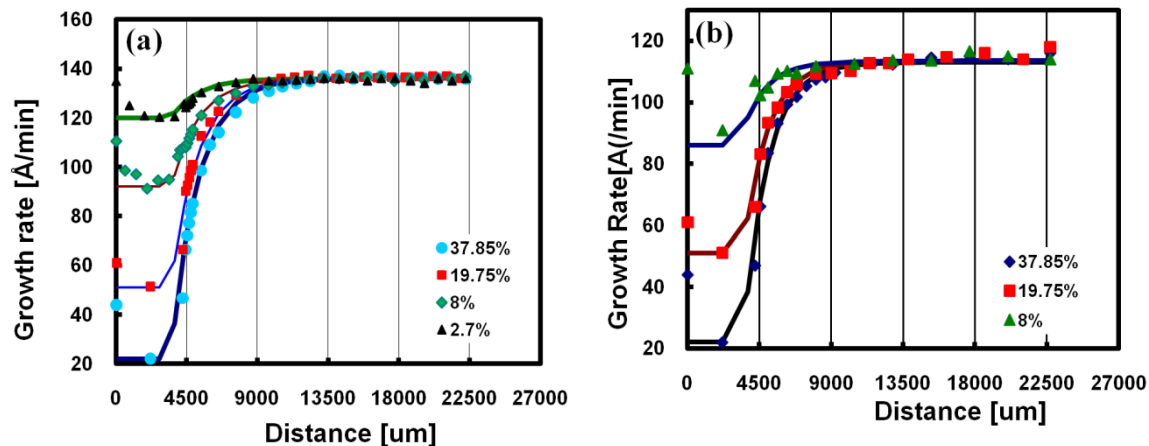


Figure 8. The measured (dots) and calculated (lines) growth rate of an array of openings along five chips. a) The trap (first chip from left) has an exposed Si coverage of 2.7, 8, 19.75 and 37.85% where this value is about 1% for the surrounding chips. b) The trap has an exposed Si coverage of 8, 19.75 and 37.85% where this value is 2.7% for the surrounding chips. The applied  $P_{\text{DCS}}$ ,  $P_{\text{GeH}_4}$  and  $P_{\text{HCl}}$  partial pressures were 60, 0.9 and 20 mtorr, respectively.

### Conclusion

In this work, a detailed model to predict the growth rates and compositions of  $\text{Si}_{1-x}\text{Ge}_x$  layers grown on patterned substrates by RPCVD has been developed. It is able to explain the growth kinetics through gas phase processes and related surface reactions.

A good agreement between the model and the experimental data of the growth profile has been achieved. This model is based on different input parameters, such as dichlorosilane, germane, hydrochloric acid partial pressures, growth temperature and mask layout. The interaction between chips (sub-chips) on a wafer was modeled using a new approach.

### Acknowledgments

This work was supported by Semiconductor Research Corporation (SRC).

### References

1. K. Goto, J. Murota, T. Maeda, R. Schutz, K. Aizawa, R. Kircher, K. Yokoo, and S. Ono, *Jpn. J. Appl. Phys.*, **32**, 438 (1993).
2. S. Verdonckt-Vandebroek, E. F. Crabbe, B. S. Meyerson, D. L. Hame, P. J. Restle, J. M. C. Stork, and J. B. Johnson, *IEEE Trans. Electron Devices*, **41**, 90 (1994).
3. A.-C. Lindgren, P.-E. Hellberg, M. von Haartman, D. Wu, C. Menon, S.-L. Zhang, and M. Östling, *Proceedings of the ESSDERC*, (unpublished), p. 175 (2002).
4. S.E. Thompson, G. Sun, K. Wu, J. Lim, T. Nishida, *IEEE Trans. on Electron Devices*, **51**, 1790 (2004).
5. Ghani T et al, *IEDM Tech Digest*, **978** (2003).
6. S. Gannavaram, N. Pesovic, M.C. Ozturk, Technical Digest - *International Electron Devices Meeting*, 437-440 (2000).
7. TH. J. M. Kuijter, L. J. Giling and J. Bloem, *Journal of Crystal Growth*, **22**, 29-33 (1974).
8. K.L. Knutson, R.W. Carr, W.H. Liu, S.A. Campbell, *Journal of Crystal Growth*, **140**, 191-204 (1994).

9. Bhavesh Mehta and Meng Tao, *Journal of The Electrochemical Society*, **152**, 4, G309-G315 (2005).
10. S. Bodnar, E. de Berranger, P. Bouillon, M. Mouis, T. Skotnicki, J.L. Regolini, *J. Vac. Sci. Technol. B: Microelectronics Processing and Phenomena*, **15**, 712 (1997).
11. T.I. Kamins, *Journal of Applied Physics*, **74**, 5799 (1993).
12. W.B. De Boer, D. Terpstra, R. Dekker, *Materials Research Society Symposium Proceedings*, **533**, 315-320 (1998).
13. L. Vescan, *Materials Science & Engineering B*, **28**, 1-8 (1994).
14. R. Loo, M. Caymax, *Applied Surface Science*, **224**, 24-30 (2004).
15. J.Hållstedt, E. Suvar, C. Menon, P.-E. Hellstrom, M. Ostling, H.H. Radamson, *Materials Science and Engineering B: Solid-State Materials for Advanced Technology*, **109**, 122-126 (2004).
16. J. Hållstedt, M. Kolahdouz, R. Ghandi and H. H. Radamson, *Journal Of Applied Physics*, **103**, 054907 (2008).
17. M. Kolahdouz, J. Hållstedt, A. Khatibi, M. Östling, R. Wise, D. J. Riley, .H. Radamson, *IEEE Transactions On Nanotechnology*, **8**, 3 (2009).
18. M. Tao, *Thin Solid Films*, **223**, 201-211 (1993).
19. M. Hierlemann, A. Kersch, C. Werner, and H. Schäfe, *J. Eteetrochem. Soc.*, **142**, 1, (1995).
20. H. Kühne, *J. Crystal Growth*, **125**, 291-300 (1992).
21. M. Kolahdouz, L. Maresca, M. Ostling, D. Riley, R. Wise, H.H. Radamson, *Solid-State Electronics*, **53**, 858–861(2009).
22. H.H. Radamson, M. Kolahdouz, R. Ghandi, J. Hållstedt, *Thin Solid Films*, **517**, 84–86 (2008).